

## Amperometric Detection of Isoprenaline Based on Glassy Carbon Electrode Modified by Iridium Oxide Nanoparticles

Mahmoud Roushani\* and Somayeh Farokhi

Department of Chemistry, Ilam University, 69315-516 Ilam, Iran

A simple and sensitive electrochemical sensor by using a glassy carbon electrode modified by iridium oxide nanoparticles (GCE/IrOxNPs) was constructed and utilized to determine isoprenaline (IP). This sensor was used successfully for IP determination in human urine samples. IrOxNPs are grown on a GCE by electrodeposition method. Various experimental parameters influencing the electrochemical behavior of the modified electrode were optimized by varying the scan rates and pH. Compared with a bare GCE, the GCE/IrOxNPs exhibits a distinct shift of the oxidation potential of IP in the cathodic direction and a marked enhancement of the current response. The results showed that GCE/IrOxNPs exhibited excellent electrochemical activity towards IP in pH 7.0 phosphate buffer solution (PBS). The detection limit, sensitivity and catalytic rate constant ( $k_{cat}$ ) of the modified electrode toward IP were  $90 \text{ nmol L}^{-1}$ ,  $17.3 \text{ nA } \mu\text{mol}^{-1} \text{ L}$  and  $1.6 \times 10^4 \text{ mol}^{-1} \text{ L s}^{-1}$ , respectively, at linear concentration rang up to  $2500 \mu\text{mol L}^{-1}$ . The modified electrode displayed linear responses to IP in amperometry assays in real urine, with a detection limit of  $120 \text{ nmol L}^{-1}$ .

**Keywords:** isoprenaline, nano-iridium oxide, chemical modified electrode, electrocatalytic

### Introduction

Isoprenaline or isoproterenol (IP) (trade names Medihaler-Iso and Isuprel) is a medication used for the treatment of bradycardia (slow heart rate), heart block, and rarely for asthma. It is a non-selective beta-adrenergic agonist and structurally similar to adrenaline.<sup>1</sup> The cardiovascular effects of IP are compared with the epinephrine and norepinephrine, which can relax almost every kind of the smooth musculature that contains adrenergic nervous, but this effect is pronounced in the musculature of bronchus and also in the gastrointestinal tract. The IP is better absorbed when dispensed by inhalation.<sup>2</sup>

A variety of methods have been used for determining IP in tablets and biological fluids, for example fluorescence,<sup>3</sup> spectrophotometric,<sup>4</sup> nuclear magnetic resonance spectroscopy,<sup>5</sup> and chemiluminescence.<sup>6</sup> Electrochemical analytical methods have been attracting considerable attention in the field of drug analysis, with the last few decades having witnessed modification of the electrode surface using a variety of nanomaterials for effective determination of the electroactive species of interest.

In comparison with the conventional techniques for IP determination, electrochemistry based on a modified

electrode show the advantages of low cost, easy preparation, rapid detection, low consumption, high selectivity and sensitivity.<sup>7-17</sup> No study is reported in the literature on the electrocatalytic determination of isoproterenol using nanosized metal and metal oxide nanostructures modified electrodes.

Design, fabrication and application of novel electrochemical sensors have been a topic of research in recent years.<sup>18,19</sup> Recently, more attention has been focused on the synthesis and application of nanoparticles (NPs), since they have properties such as high electrical conductivity, high surface area and chemical stability.<sup>20-22</sup>

NPs can be used to promote electron transfer reactions when used as electrode material in electrochemical device. Therefore, modification of electrochemical interface with nanosized metal and metal oxide nanostructures is one of the recent approaches used extensively in the development of sensing platforms.<sup>23</sup>

In comparison to other metal oxide based modified electrodes, iridium oxide nanoparticles (IrOxNPs) is a stable metal oxide with excellent electrochemical reversibility at wide pH range.<sup>24</sup> It is a good candidate for many applications such as preparation of clinical diagnostics devices,<sup>25</sup> power sources,<sup>26</sup> electrochromic devices,<sup>27</sup> oxygen reduction,<sup>28</sup> pH sensing,<sup>29</sup> and sensors and biosensors fabrication.<sup>30-32</sup> Furthermore, due to high

\*e-mail: mahmoudroushani@yahoo.com

electron transfer rate constant of Ir<sup>IV</sup>/Ir<sup>III</sup> redox couple, it can act as electron transfer mediator for electrocatalytic processes and electroanalysis.<sup>21,24,30-34</sup> We report here on the use of a glassy carbon electrode modified by iridium oxide nanoparticles (GCE/IrO<sub>x</sub>NPs) as an amperometric sensor for the electrocatalytic oxidation of an IP. The prepared IrO<sub>x</sub>NPs has been used as an excellent catalyst for IP oxidation at lower overpotentials. Cyclic voltammetry and amperometry have been used for the investigation of the electrochemical properties and electrocatalytic activity of the nanoparticle-modified electrode. The fabricated sensor was used for the detection of nanomolar concentrations of an IP and linear concentration range at pH 7, using hydrodynamic amperometry. To the best of our knowledge, up to now, there is no report on the application of GCE/IrO<sub>x</sub>NPs to the detection of IP.

## Experimental

### Reagents and apparatus

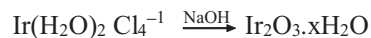
Isoprenaline, IrCl<sub>3</sub>·xH<sub>2</sub>O and other reagents were purchased from Merck and used without purification. The buffer solutions (0.1 mol L<sup>-1</sup>) were made from Na<sub>3</sub>PO<sub>4</sub>, NaH<sub>2</sub>PO<sub>4</sub> and Na<sub>2</sub>HPO<sub>4</sub> and the pH was adjusted with 0.1 mol L<sup>-1</sup> H<sub>3</sub>PO<sub>4</sub> or 1.0 mol L<sup>-1</sup> NaOH. The pH was measured with a Metrohm model 780 pH/mV meter. Solutions were deaerated by bubbling high purity (99.99%) N<sub>2</sub> gas through them prior to the experiments. All electrochemical experiments were carried out at a temperature of 25 ± 0.1 °C.

All the electrochemical experiments were performed on a μ-AUTOLAB type III and FRA2 board computer controlled Potentiostat/Galvanostat (Eco-Chemie, The Switzerland) driven with NOVA software. A conventional three-electrode cell was used with a Ag/AgCl/(sat. KCl) reference electrode, a Pt wire as the counter electrode and a GC disk (modified and unmodified) as the working electrode. Cyclic voltammetry was used for the modification of GCE/IrO<sub>x</sub>NPs based on the reported procedure.<sup>35</sup> Scanning electron microscopy (SEM) imaging is used for the study of modified surfaces morphology.

### Modification of GCE

The deposition solution of iridium was prepared pursuant to a two-step procedure carried out by Baur.<sup>36</sup> The first step in the preparation of this solution is the formation of the diaquaetetrachloroiridate(III) ion, Ir(H<sub>2</sub>O)<sub>2</sub>Cl<sub>4</sub><sup>-1</sup> from K<sub>3</sub>IrCl<sub>6</sub>. Accordingly, a 1 mmol L<sup>-1</sup> solution of IrCl<sub>6</sub><sup>-3</sup> in 0.1 mol L<sup>-1</sup> HCl was aquated by

heating at 80 °C for 2 h. The second step in the preparation of the deposition solution is the formation of Ir<sup>III</sup> oxide from Ir(H<sub>2</sub>O)<sub>2</sub>Cl<sub>4</sub><sup>-1</sup> with added base according to following reaction:



Prior to the addition of base, oxygen must be removed because the iridium(III) oxide is unstable in oxygen. After removing the oxygen from the acidic solution of Ir(H<sub>2</sub>O)<sub>2</sub>Cl<sub>4</sub><sup>-1</sup>, the pH of solution was raised to 10.5 by adding anhydrous potassium carbonate. Prior to modification, the bare GCE (2 mm in diameter) was polished successively with alumina on a polishing cloth and then rinsed with doubly distilled water. Then, the clean electrode was immersed in the solution containing iridium(III) oxide and cyclic voltammograms recorded with 20 cycling of the potential from 0.1 to 1.2 V at scan rate 50 mV s<sup>-1</sup>. GCE modified with IrO<sub>x</sub> layers were cleaned with distilled water and used for other applications as detailed below.

## Results and Discussion

### Surface characterization and electrochemical behavior investigation of the modified electrode

Scanning electron microscopy was used to characterize the surface morphologies of different electrodes. Figure 1 shows the SEM of bare GCE (Figure 1a) and GCE/IrO<sub>x</sub> (Figure 1b). As shown, a uniformly distributed thin film of

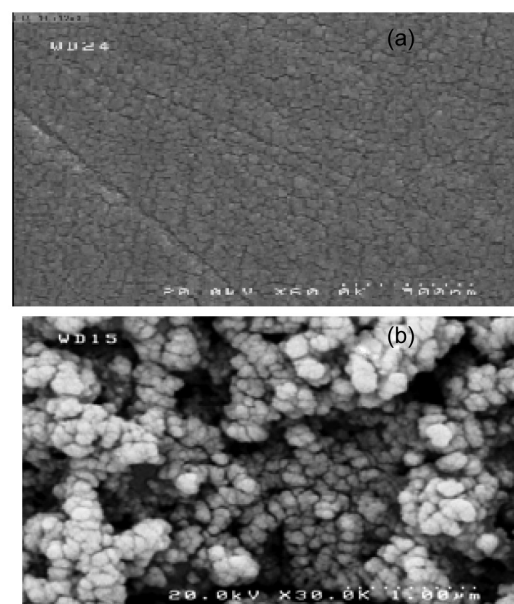


**Figure 1.** Scanning electron microscopy of (a) bare GCE and (b) GCE/IrO<sub>x</sub>.

iridium oxide particles with an average diameter ranging from 50 to 100 nm has grown on the GCE surface.

The electrochemical behavior of the modified electrode was investigated by recording its cyclic voltammograms in pH 7 buffer solution (Figure 2). As expected, the cyclic voltammogram displays a reversible redox system at  $E_{1/2} = 0.245$  V vs. reference electrode assigned to one electron redox process,  $\text{Ir}^{\text{III}}/\text{Ir}^{\text{IV}}$ .<sup>29</sup> Figure 2 shows the cyclic voltammograms of the modified electrode at different scan rates in the potential range of  $-0.2$ - $0.6$  V in pH 7 buffer solution. As illustrated in the inset of Figure 2, the peak currents increased linearly with the scan rate as expected for the thin layer electrochemistry process. Moreover, the anodic peak currents are almost the same as the corresponding cathodic peak currents. The peak-to-peak potential separation is about 18 mV for sweep rates below  $100$   $\text{mV s}^{-1}$ , suggesting facile charge transfer kinetics over this range of sweep rate.

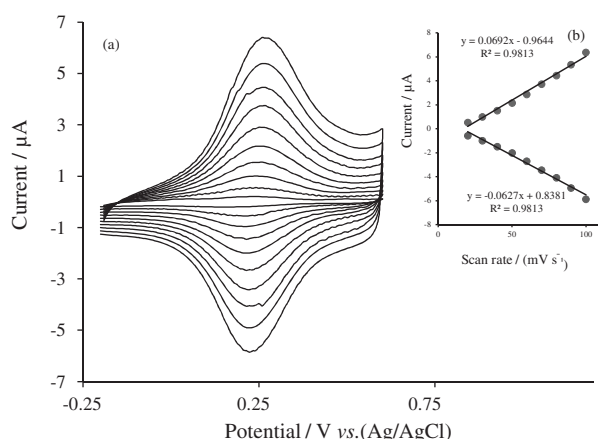
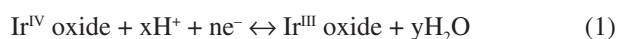


**Figure 2.** (a) Cyclic voltammetric responses of a GCE/IrOxNPs in PBS (pH 7) at scan rates (inner to outer) of 20, 30, 40, 50, 60, 70, 80, 90, and  $100$   $\text{mV s}^{-1}$ . (b) Plots of peak currents vs. the scan rate.

The electrochemical properties and pH response of the GCE/IrOxNPs modified electrode with electrodeposited iridium-oxide nanoparticles were investigated in the author's previous report.<sup>21</sup> To study the effect of pH on the electrochemical behavior of the GCE modified with iridium oxide films, the cyclic voltammograms of the modified electrode were recorded in electrolyte solutions over the pH range 6-13. Figure 3 shows the results at a scan rate of  $50$   $\text{mV s}^{-1}$ . To account for the electrochemical behavior, the general reaction for the pH sensitivity of iridium oxide electrodes can be written as follows:<sup>35,36</sup>



where values of  $n$ ,  $x$  and  $y$  vary with the oxide preparation method and are usually not integers.<sup>36</sup> The inset of Figure 3

shows the plot of formal potential ( $E_0$ ) vs. pH for GCE modified with IrOx thin films; the slope of this plot is about  $79$  mV *per* decade; similar results were observed for other electrode materials modified by iridium oxide layers.<sup>37-39</sup> The GCE modified with IrOx layers can be used as electrodes for pH sensing for practical applications because the IrOx films exhibit high stability both in acidic and alkaline solutions.

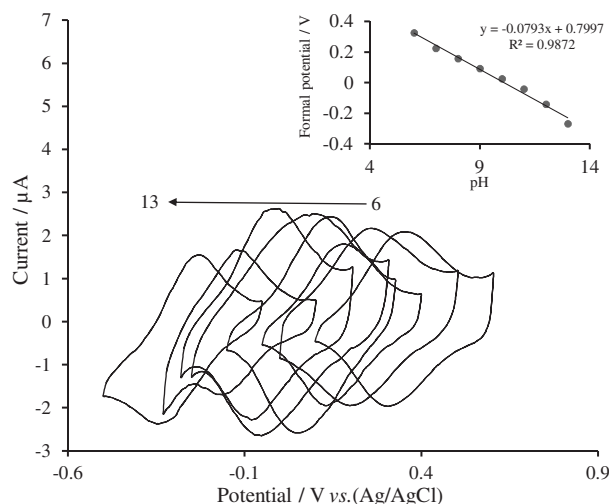


**Figure 3.** Cyclic voltammetric response of the GCE/IrOxNPs at a pH of 6, 7, 8, 9, 10, 11, 12 and 13 (from right to left) at a scan rate of  $50$   $\text{mV s}^{-1}$ . The inset shows the variation of formal potential vs. pH values.

The surface coverage ( $\Gamma$ ) of IrOx films was evaluated from the following equation:

$$\Gamma = Q/nFA \quad (2)$$

where  $Q$  is the charge obtained by integrating the anodic peak at low voltage scan rates, and the other symbols have their usual meaning. In the present case, the calculated value of  $\Gamma$  is  $7.5 \times 10^{-9}$  mol  $\text{cm}^{-2}$ . The surface coverage value for the GCE/IrOxNPs was  $7.5 \times 10^{-9}$  mol  $\text{cm}^{-2}$ , which corresponds to the presence of multilayer of surface species. These results indicate high ability of the IrOx NPs for oxidation of IP.

#### Electrocatalytic oxidation of IP at GCE/IrOxNPs

IrOx modified electrodes have been used for pH sensing due to electrochemical activity and stability of redox couple at wide pH range, 1-11.<sup>37</sup> Furthermore, because of electrochemical reversibility and high electron transfer rate constant of the  $\text{Ir}^{\text{III}}/\text{Ir}^{\text{IV}}$  redox couple at wide pH range, it can be used as mediator for shuttle electrons between electrodes and analytes.<sup>40</sup> One of the main objectives of this work was to fabricate a modified electrode capable

of the electrocatalytic oxidation of IP. In order to examine the electrocatalytic activity of the modified electrodes, the cyclic voltammograms were obtained in the presence and absence of IP at bare and modified electrodes. Figure 4 shows the recorded cyclic voltammograms of the modified and bare GCE in the presence and absence of IP in phosphate buffer solution (PBS) (pH 7). Cyclic voltammetric studies showed that the oxidation of IP at modified electrode occurs at a potential about 220 mV less positive than at unmodified GCE and a catalytic peak current of GCE/IrOxNPs was amplified by approximately 2 times in comparison with the bare GCE, indicating a strong catalytic effect. Thus, reduced oxidation peak potential and enhanced peak current for IP oxidation are achieved with the modified electrodes.

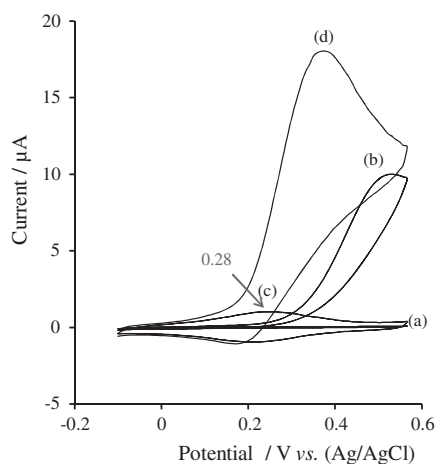


**Figure 4.** Measured cyclic voltammograms of (a) GCE in 0.1 mol L<sup>-1</sup> PBS pH 7.0 at scan rate of 30 mV s<sup>-1</sup> and (b) in the presence of 1.6 mmol L<sup>-1</sup> IP (c) and (d) are same results as (a) and (b) for GCE/IrOxNPs.

In order to optimize the electrocatalytic response of modified electrodes toward IP oxidation, the effect of pH on the catalytic oxidation behavior was investigated. The cyclic voltammograms of IrOx film modified GCE in 0.19 mmol L<sup>-1</sup> IP concentration at different pH value (6-13) were recorded (Figure 5). By decreasing the pH values, the oxidation peak potential shifts to more positive value and the peak current is increased. Since more reproducible results and high catalytic activity of modified electrode was observed at pH 7, we chose this pH as optimum value for IP determination.

The effect of IP addition to the system was investigated in the range of 0.2-1.9 mmol L<sup>-1</sup> (Figure 6), fitting a linear dependence of currents vs. concentration of IP, which fitted the equation  $I (\mu\text{A}) = 12.515 (\mu\text{A mmol}^{-1} \text{L}) + 1.2735 (\mu\text{A})$  and  $R^2 = 0.99$ . As shown in Figure 6, the anodic peak currents are increased and cathodic peak currents unchanged with increasing the IP concentration.

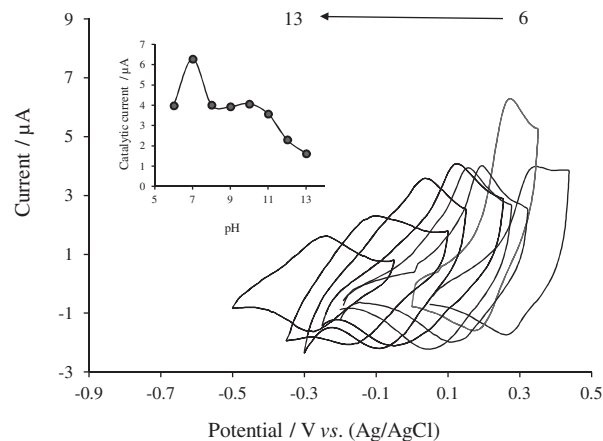


**Figure 5.** Cyclic voltammograms of the GCE/IrOxNPs in different pH solutions, from right to left, 6 to 13, in the presence of 0.19 mmol L<sup>-1</sup> of IP and scan rate of 50 mV s<sup>-1</sup>. Inset: plot of peak current vs. pH values.

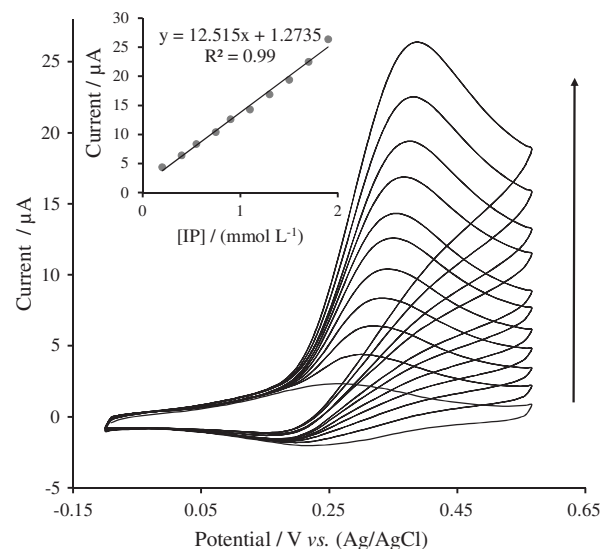
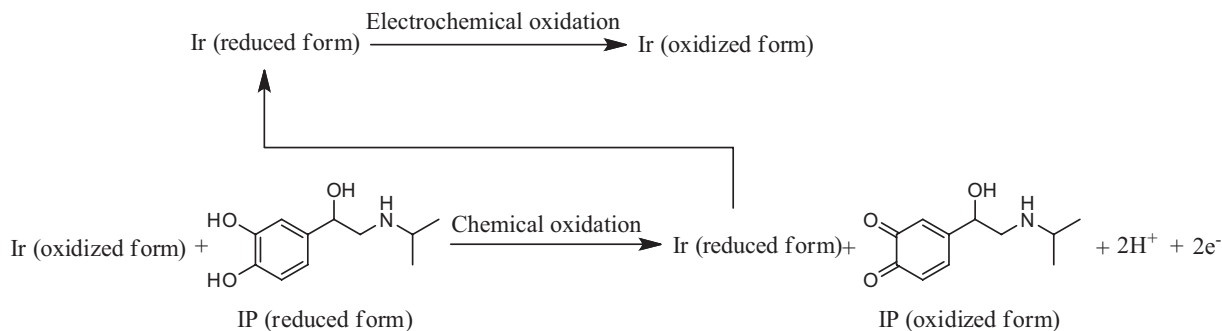


**Figure 6.** Cyclic voltammograms of GCE/IrOxNPs in PBS pH 7.0 at scan rate 50 mV s<sup>-1</sup> with increasing IP concentration (from inner to outer) 0.2, 0.4, 0.55, 0.75, 0.9, 1.1, 1.3, 1.5, 1.7 and 1.9 mmol L<sup>-1</sup>. Inset: plot of peak current vs. IP concentrations.

For the investigation of the electrocatalytic mechanism of the modified electrode toward IP oxidation, cyclic voltammograms of modified electrode in 2 mmol L<sup>-1</sup> IP at different scan rates were recorded (not shown). The peak current for the anodic oxidation of IP was proportional to the square root of the scan rate, suggesting that the process is controlled by diffusion of analyte as expected for a catalytic system. In addition, a plot of the scan rate-normalized current ( $I_p/v^{1/2}$ ) vs. scan rate exhibited the characteristic shape of a typical EC' catalytic process. During the anodic scan, the Ir<sup>III</sup> present in the mediator is electrochemically oxidized to Ir<sup>IV</sup>, which in turn chemically oxidizes the IP (reduced form) present in the solution to IP (oxidized form) and getting itself reduced to Ir<sup>III</sup>. The Ir<sup>III</sup> is again reoxidized to Ir<sup>IV</sup>, at the electrode surface,



Scheme 1.

which again oxidizes IP (reduced form) chemically, and this process is repeated a number of times, resulting in electrocatalytic oxidation of IP by the mediator present in the modified electrode.

Based on these results, the reaction sequence in the oxidation of IP by IrOx redox couple can be described by Scheme 1.

For an EC' mechanism, Andrieux and Saveant<sup>41</sup> theoretical model can be used to calculate the catalytic rate. Based on this model, for a slow scan rate and a large catalytic rate, the relationship between the peak current and the analyte concentration reads:

$$I_p = \alpha n F A D^{1/2} \left( \frac{\nu F}{RT} \right)^{1/2} C_s \quad (3)$$

where  $D$  and  $C_s$  are the diffusion coefficient ( $\text{cm}^2 \text{s}^{-1}$ ) and the bulk concentration ( $\text{mol cm}^{-3}$ ) of substrate (IP), respectively, and other symbols have their usual meanings. Low values of  $K_{\text{cat}}$  result in values of the coefficient lower than 0.496. For low scan rates ( $5\text{--}20 \text{ mV s}^{-1}$ ), the average coefficient value ( $\alpha$ ) in equation 4 is found to be 0.32 for a GCE/IrOxNPs, with a surface coverage of  $7.5 \times 10^{-9} \text{ mol cm}^{-2}$  and a geometric area  $A$  of  $0.12 \text{ cm}^2$  in  $2 \text{ mmol L}^{-1}$  IP at pH 7.0. According to the approach of Andrieux and Saveant<sup>41</sup> and using the values found in Figure 1 of their work, the average values of the calculated  $K_{\text{cat}}$  are  $1.6 \times 10^4 \text{ mol}^{-1} \text{ L s}^{-1}$  for modified electrode. The high  $K_{\text{cat}}$  obtained for GCE/IrOxNPs implies that this system can be efficiently used as electrochemical sensor for IP detection.

#### Amperometric detection of IP at modified electrode

Amperometric method shows a lower background current that arises primarily from full charging the electrochemical double-layer capacitance in a short time scale, due to the fact of the potential of the working electrode is fixed during time. Constant potential amperometry is an electrochemical technique where a constant potential is

applied to a sensor (working electrode) and the faradaic current is measured. This current is generated by the reduction or oxidation of the target chemical substance (analyte) at the electrode surface. According to the potential dependence of the IP electrocatalytic oxidation current under steady-state conditions, the optimum electrode potential was selected at  $0.28 \text{ V}$  versus the Ag/AgCl reference electrode in order to obtain constant and high sensitivity. As discussed above, the proposed modified electrode showed excellent and strong mediation properties to facilitate the low potential amperometric measurements of IP. Figure 7a shows a typical current-time plot of the rotated modified GCE (rotation speed  $1000 \text{ rpm}$ ) on successive additions of  $15 \mu\text{mol L}^{-1}$  and  $285 \mu\text{mol L}^{-1}$  of IP at an applied potential of  $0.28 \text{ V}$  (vs. Ag/AgCl). As shown, the modified electrode responded rapidly and approached 97% of the steady-state current within 3 s. Figure 7f shows a typical current-time plot of the rotated GCE (rotation speed  $1000 \text{ rpm}$ ) on successive additions of  $99 \mu\text{mol L}^{-1}$  and  $1386 \mu\text{mol L}^{-1}$  of IP at an applied potential of  $0.28 \text{ V}$  (vs. Ag/AgCl). As shown, the bare GCE has a rapid decay of the signal.

The plot of current response vs. IP concentration is shown in Figures 7a and 7c. The calibration plot is linear over a wide concentration range ( $1 \mu\text{mol L}^{-1}$  to  $2500 \mu\text{mol L}^{-1}$ ), while for a high concentration of IP, the plot of current vs. analyte concentration deviates from linearity (Figure 7c). The linear least squares calibration curve over the range of  $15\text{--}285 \mu\text{mol L}^{-1}$  (19 points) is  $I (\mu\text{A}) = 0.0173 [\text{IP}] \mu\text{mol L}^{-1} + 0.1459 \mu\text{A}$  with a correlation coefficient of 0.9985, indicating that the regression line fits very well with the experimental data and the regression equation can be applied in the unknown sample determination. The detection limit (when signal to noise ratio was 3) and sensitivity were  $0.09 \mu\text{mol L}^{-1}$  and  $17.3 \text{ nA } \mu\text{mol L}^{-1}$ , respectively. Highly stable amperometric response toward IP is an extremely attractive feature of the modified GCE. Figure 7e shows the amperometric response of  $99 \mu\text{mol L}^{-1}$  IP during a prolonged 44 min

experiment. The response remains stable throughout the experiment (only a 1% decrease in current was observed), indicating that the GCE/IrOxNPs imparts higher stability for amperometric measurements of IP. Thus the GCE/IrOxNPs was found to exhibit very high sensitivity and a fast response time for IP detection.

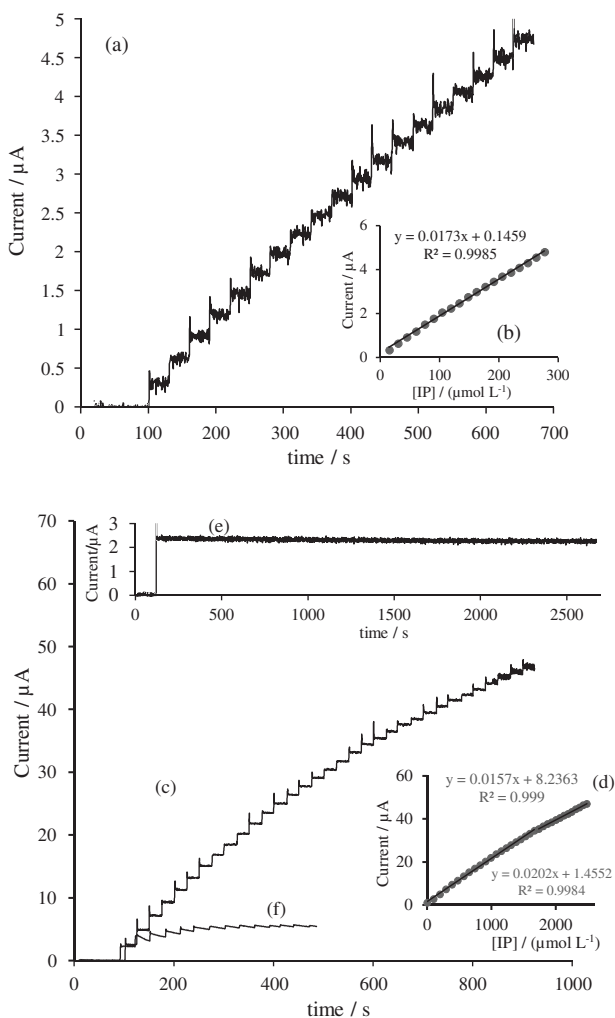


**Figure 7.** Amperometric response at the rotating GCE/IrOxNPs (rotation speed 1000 rpm) held at 0.28 V in PBS (pH 7) for successive additions of (a) 15  $\mu\text{mol L}^{-1}$  and (c) 99  $\mu\text{mol L}^{-1}$  IP and (b) and (d) calibration curves for variation of current vs. IP concentrations. (e) The recorded chronoamperogram for 99  $\mu\text{mol L}^{-1}$  IP during long period time (44 min). (f) Amperometric response at a rotating unmodified GCE for successive addition of 99  $\mu\text{mol L}^{-1}$  IP, other conditions as (c).

Application of the modified electrode for determination of IP in real sample and study of the selectivity of the sensor

In order to examine the capability of our sensor for determination of IP in real specimens, we measured the concentration of IP in an artificially prepared specimen, prepared as follows. A 0.1 mol  $\text{L}^{-1}$  PBS (pH 7.0) was prepared using urine samples and IP was added to obtain

a solution with concentration of 68  $\mu\text{mol L}^{-1}$  IP. The standard addition method was used for determination of IP in this specimen. The recorded chronoamperograms of the modified electrode in this specimen for different concentration of IP is shown in Figure 8a. The calibration curve (as shown in Figure 8b) is obtained as  $I_p(\mu\text{A}) = 0.0331 [\text{IP}] (\text{mmol L}^{-1}) + 2.21$  ( $\mu\text{A}$ ) with a correlation coefficient of 0.996. Using the intercept point of this equation with the concentration axis, the concentration of IP in the real sample is obtained as  $67 \pm 1 \mu\text{mol L}^{-1}$ , which is very close to the real concentration of initial IP (68  $\mu\text{mol L}^{-1}$ ) in the solution, confirming the capability of our sensor for determination of IP in the real specimens. This procedure was repeated five times and the relative standard deviation was calculated as 2.1%. Different standard concentrations of IP were added to the diluted solution of IP injection sample. Then, the IP contents were measured. The results showed good recoveries between 96% and 102% ( $n = 4$ ). For the urine samples, each sample was analyzed in triplicate by standard addition method using the proposed method. The samples were centrifuged and diluted five times with water without any further pretreatment. The recovery ratio indicates that the determination of IP using the modified electrode is effective and can be applied for their detection of IP in real samples.

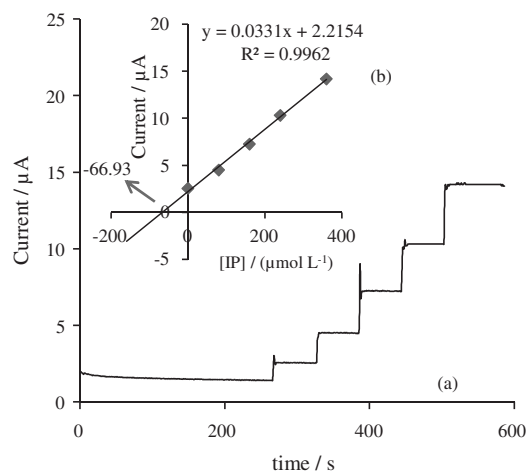


**Figure 8.** (a) Amperometric response of GCE/IrOxNPs (rotation speed 1000 rpm) held at 0.28 V in PBS (pH 7), and in real sample pH 7 in the presence of different concentrations of IP (0, 80, 160, 240 and 320  $\mu\text{mol L}^{-1}$ ). (b) Plot of currents ( $I_a$ ) vs. IP concentration.

The chronoamperograms of the modified electrode in response to increasing concentrations of IP in synthetic urine was very similar to that of the sensor in PBS. Thus, no interference in the sensor, related to synthetic urine, was observed. This suggests that the sensor would be capable of selective and specific detection of IP in real urine samples. Figure 9 shows a typical hydrodynamic

amperometric response obtained by successfully adding IP to a continuously stirred modified electrode (rotation speed 1000 rpm) in synthetic urine. As shown in Figure 9, during the successive addition of  $15 \mu\text{mol L}^{-1}$  of IP, a well-defined response was observed. The measured currents increase, as the IP concentration in solution is increased. The calibration plot for IP determination was linear for a wide range  $15 \mu\text{mol L}^{-1}$ - $1800 \mu\text{mol L}^{-1}$ . Linear least square calibration curves over the range  $15$ - $315 \mu\text{mol L}^{-1}$  (by 21 determinations) had a slope of  $5.6 \text{ nA } \mu\text{mol L}^{-1}$  (sensitivity) and a correlation coefficient  $0.9967$ . The detection limit was  $120 \text{ nmol L}^{-1}$  when the signal to noise ratio was 3.

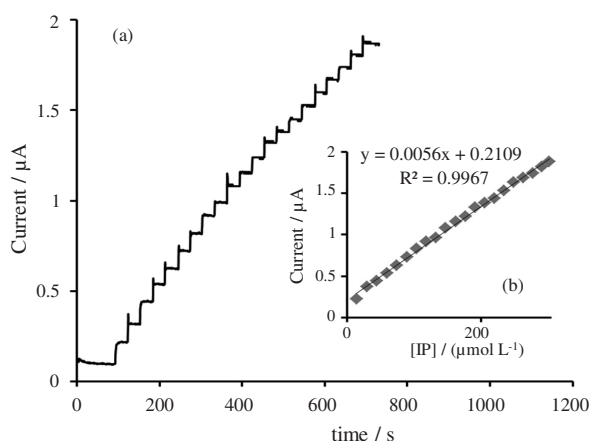


**Figure 9.** (a) Amperometric response of GCE/IrOxNPs (rotation speed 1000 rpm) held at  $0.28 \text{ V}$  in real sample pH 7 for successive additions of  $15 \mu\text{mol L}^{-1}$  IP. (b) Plot of currents ( $I_a$ ) vs. IP concentration.

The selectivity of the prepared modified electrode was studied toward determination of IP. For this purpose, the influence of various foreign species on the determination of IP was investigated. Figure 10 shows amperometric response of the rotated modified electrode for IP in the presence of several interference in buffer solution, pH 7. As can be seen, no response is observed for modified electrode in the presence of different interfering substances. The maximum concentrations of foreign substances, which did not interfere the determination of IP were 10-fold excess of  $\text{Na}^+$ ,  $\text{K}^+$ , glucose, L-serine, L-glycine, tryptophan, L-alanine, methadone, ascorbic acid, uric acid and pethidin. Furthermore, the electrode response for IP was not changed after adding interfering substances. The selectivity and the anti-interference advantages of the sensor are largely attributed to the low operating potential used in the determination. Working point, detection limit, linear calibration range and pH of the proposed modified electrode were compared with those previously reported, and the results are summarized in Table 1. The results above demonstrate that GCE/IrOxNPs has satisfactory analytical performance and it can be a feasible sensor for IP.

To check the reproducibility of the GCE/IrOxNPs, a series of four electrodes fabricated in a same manner were employed for the detection of  $300 \mu\text{mol L}^{-1}$  IP in  $0.1 \text{ mol L}^{-1}$  PBS (pH 7). A relative standard deviation (RSD) of the peak current values obtained at the five electrodes was  $2.3\%$ , suggesting good reproducibility of the proposed electrode (Figure 11).

**Table 1.** Analytical parameters for IP at several modified electrodes

Modified electrode	Methodology	Working point / V	pH	Linear range / ( $\mu\text{mol L}^{-1}$ )	Limit of detection / ( $\mu\text{mol L}^{-1}$ )	Reference
CuHCF <sup>a</sup> /CP <sup>b</sup>	CV <sup>c</sup>	0.813	6	196-1070	80	7
FMAMCNTPE <sup>d</sup>	DPV <sup>e</sup>	0.45	5	0.5-50	0.2	8
PDNA <sup>f</sup> /GCE	CV	0.416	4	2-60	0.16	9
p-CACNTPE <sup>g</sup>	DPV	0.1	10.5	0.015-100	0.009	10
MWCNTIL <sup>h</sup> /CP	DPV	0.47	6	1-520	0.85	11
Graphene/GCE	CV	0.413	4	0.21-100	0.064	12
DHPB <sup>i</sup> /MWCNTs/CP	SWV <sup>j</sup>	0.3	7	0.3-125	0.1	13
5ADB <sup>k</sup> /CNTs/CP	SWV	0.28	7	0.4-900	0.2	14
PNH <sup>l</sup> /OCNT <sup>m</sup> /CP	DPV	0.11	8	1-1800	0.3	15
Poly-ACBK <sup>n</sup> /GO-nafion/GCE	LSV <sup>p</sup>	0.52	3	0.0095-0.095	0.007	16
DHB <sup>q</sup> /CNTs/CP	DPV	0.27	7	10-6000	1.24	17
IrOxNPs/GCE	Amp <sup>q</sup>	0.28	7	1-2500	0.09	This work

<sup>a</sup>Copper(II) hexacyanoferrate(III); <sup>b</sup>carbon paste; <sup>c</sup>cyclic voltammetry; <sup>d</sup>ferrocenemonocarboxylic acid modified carbon nanotubes paste electrode; <sup>e</sup>differential pulse voltammetry; <sup>f</sup>poly(1-methylpyrrole)-DNA; <sup>g</sup>p-chloranil-carbon nanotubes paste electrode; <sup>h</sup>multiwall carbon nanotubes ionic liquid; <sup>i</sup>N-(3,4-dihydroxyphenethyl)-3,5-dinitrobenzamide; <sup>j</sup>square wave voltammetry; <sup>k</sup>5-amino-3',4'-dimethyl-biphenyl-2-ol; <sup>l</sup>2,2'-[1,4-phenylenediyl-bis(nitrilomethylidene)]-bis(4-hydroxyphenol); <sup>m</sup>oxidized multiwall carbon nanotubes; <sup>n</sup>acid chrome blue K; <sup>o</sup>linear sweep voltammetry; <sup>p</sup>2-((7-(2,5-dihydrobenzylideneamino)heptylimino)methyl)benzene-1,4-diol; <sup>q</sup>amperometry.

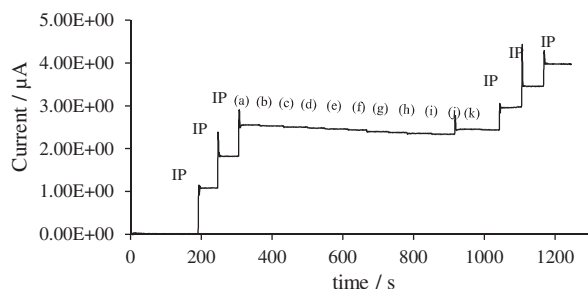


**Figure 10.** Amperometric response of GCE/IrOxNPs (rotation speed 1000 rpm) at an applied potential of 0.28 V in PBS (pH 7) for the successive addition of  $99 \mu\text{mol L}^{-1}$  of IP and  $1 \text{ mmol L}^{-1}$   $\text{Na}^+$  (a),  $\text{K}^+$  (b), glucose (c), L-serine (d), L-glycine (e), uric acid (f), tryptophan (g), L-alanine (h), methadone (i),  $0.5 \text{ mmol L}^{-1}$  of ascorbic acid (j), and pethidin (k).

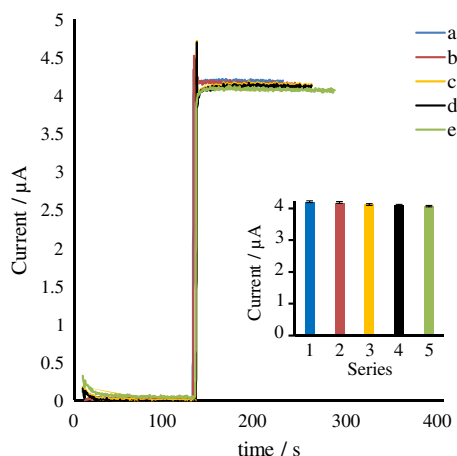


**Figure 11.** Amperometric response for five series of GCE/IrOxNPs (rotation speed 1000 rpm) at an applied potential of 0.28 V in PBS (pH 7) containing  $300 \mu\text{mol L}^{-1}$  of IP. Inset: plot of currents ( $I_a$ ) vs. series.

To evaluate the precision of the method, the analytical performance was observed for six repeated measurements of  $0.01 \text{ mmol L}^{-1}$  IP solution. A RSD of 2.4% confirmed the good precision of the method. The cyclic voltammetry (CV) response of the modified electrode was also investigated after 7 days for the same drug concentration, during which the peak current did not vary much indicating appreciable stability of the GCE/IrOxNPs.

## Conclusions

In conclusion, this paper clearly illustrates a simple and reproducible preparation technique used for the modification of GCE/IrOxNPs. The electrochemical behavior of the modified electrode was investigated by CV, and it was found that the use of potential cycling ensures excellent mechanical stability and electrochemical reproducibility of the deposited electrocatalyst. The oxidation of IP is catalyzed at pH 7.0 at GCE/IrOxNPs, whereas the peak potential of IP is shifted by 220 mV to a less positive potential rather than bare GCE.

GCE/IrOxNPs were used for the fast amperometric detection of IP at micromolar concentrations. The method is simple, fast and sensitive and is promising for routine analysis of ultra-trace amounts of IP.

## References

- Shen, H.; *Illustrated Pharmacology Memory Cards: PharMnemonics*, Minireview, **2008**, 5.
- Voet, D.; Voet, J. G.; *Biochemistry*, 2<sup>nd</sup> ed.; Wiley: New York, 1995.
- Wang, Z. P.; Zhang, Z. J.; Fu, Z. F.; Fang, L. Q.; Luo, W. F.; Chen, D. L.; Zhang, X.; *Anal. Chim. Acta* **2003**, 494, 63.
- Solich, P.; Polydorou, C. K.; Koupparis, M. A.; Efstathiou, C. E.; *J. Pharm. Biomed. Anal.* **2000**, 22, 781.
- Talebpour, Z.; Haghgo, S.; Shamsipur, M.; *Anal. Chim. Acta* **2004**, 506, 97.
- Zhang, C.; Huang, J.; Zhang, Z.; Aizawa, M.; *Anal. Chim. Acta* **1998**, 374, 105.
- Bonifacio, V. G.; Marcolino, L. H.; Teixeira, M. F. S.; Fatibello-Filho, O.; *Microchem. J.* **2004**, 78, 55.
- Ensafi, A. A.; Maleh, H. K.; *Int. J. Electrochem. Sci.* **2010**, 5, 1484.
- Kutluay, A.; Aslanoglu, M.; *Acta Chim. Slov.* **2010**, 57, 157.
- Ensafi, A. A.; Dadkhah, M.; Maleh, H. K.; *Colloids Surf., B* **2011**, 84, 148.
- Ensafi, A. A.; Maleh, H. K.; *Drug Test. Anal.* **2011**, 3, 325.
- Chen, M.; Ma, X.; Li, X.; *J. Solid State Electrochem.* **2012**, 16, 3261.
- Ensafi, A. A.; Bahrami, H.; Maleh, H. K.; Mallakpour, S.; *Chin. J. Catal.* **2012**, 33, 1919.
- Beitollahi, H.; Mohadesi, A.; Mohammadi, S.; Akbari, A.; *Electrochim. Acta* **2012**, 68, 220.
- Ardakani, M. M.; Sadrabadi, A. N.; Mohseni, M. A. S.; Naeimi, H.; Benvidi, A.; Khoshro, A.; *Electroanal. Chem.* **2013**, 705, 75.
- Lina, X.; Ni, Y.; Kokot, S.; *J. Hazard. Mater.* **2013**, 260, 508.
- Ardakani, M. M.; Sabaghian, F.; Khoshroo, A.; Naeimi, H.; *J. Catal.* **2014**, 35, 565.
- Roushani, M.; Karami, E.; Salimi, A.; Sahraei, R.; *Electrochim. Acta* **2013**, 113, 134.
- Roushani, M.; Shamsipur, M.; Pourmortazavi, S. M.; *J. Appl. Electrochem.* **2012**, 42, 1005.
- Roushani, M.; Abdi, Z.; Daneshfar, A.; Salimi, A.; *J. Appl. Electrochem.* **2013**, 43, 1175.
- Roushani, M.; Sarabaegi, M.; *J. Electroanal. Chem.* **2014**, 7718, 147.
- Roushani, M.; Abdi, Z.; *Sens. Actuators, B* **2014**, 201, 503.
- Biswas, P. C.; Nodasaka, Y.; Enyo, M.; Haruta, M.; *J. Electroanal. Chem.* **1995**, 381, 167.

24. Salimi, A.; Hyde, M. E.; Bannks, K.; Compton, R. G.; *Analyst* **2004**, *129*, 9.
25. Venkatraman, V. L.; Reddy, R. K.; Zhang, F.; Evans, D.; Ulrich, B.; Prasad, S.; *Biosens. Bioelectron.* **2009**, *24*, 3078.
26. Labou, D.; Slavcheva, E.; Schankenber, U.; Neophytides, S.; *J. Power Sources* **2008**, *185*, 1073.
27. Backholm, J. G.; Niklasson, A.; *Sol. Energy Mater. Sol. Cells* **2008**, *92*, 1388.
28. Yoshinaga, N.; Sugimoto, W.; Takasu, Y.; *Electrochim. Acta* **2008**, *54*, 566.
29. El-Giar, E. E. M.; Wipf, D. O.; *Electroanal. Chem.* **2007**, *609*, 147.
30. Hindle, P. H.; Nigro, S.; Asmussen, M.; Chen, A.; *Electrochem. Commun.* **2008**, *10*, 1438.
31. Pikulski, M.; Gorski, W.; *Anal. Chem.* **2000**, *72*, 2696.
32. Terashima, C.; Rao, T. N.; Sarada, B. V.; Spataru, N.; Fujishima, A.; *Electroanal. Chem.* **2003**, *544*, 65.
33. Salimi, A.; Alizadeh, V.; Hallaj, R.; *Talanta* **2006**, *68*, 1610.
34. Salimi, A.; Alizadeh, V.; Compton, R. G.; *Anal. Sci.* **2005**, *21*, 1275.
35. Hyde, M. E.; Compton, R. G.; *Electroanal. Chem.* **2002**, *531*, 19.
36. Baur, J. E.; Spaine, T. W.; *Electroanal. Chem.* **1998**, *443*, 208.
37. Wang, M.; Yao, S.; Madou, M.; *Sens. Actuators, B* **2002**, *81*, 313.
38. Bezbaruah, A. N.; Zhang, T. C.; *Anal. Chem.* **2002**, *74*, 5726.
39. Widf, D. W.; Spaine, F. G. W.; Baur, J. E.; *Anal. Chem.* **2000**, *72*, 4921.
40. Saterlay, A. J.; Foord, J. S.; Compton, R. G.; *Analyst* **1999**, *124*, 1791.
41. Andrieux, C. P.; Saveant, J. M.; *J. Electroanal. Chem.* **1978**, *93*, 163.

Submitted: December 19, 2014

Published online: March 20, 2015